Environmental Pollution 158 (2010) 2702–2709

Contents lists available at ScienceDirect

Environmental Pollution

journal homepage: www.elsevier.com/locate/envpol

Solving mercury (Hg) speciation in soil samples by synchrotron X-ray microspectroscopic techniques

Roberto Terzano [a,*], Anna Santoro [a], Matteo Spagnuolo [a], Bart Vekemans [b], Luca Medici [c], Koen Janssens [d], Jörg Göttlicher [e], Melissa A. Denecke [f], Stefan Mangold [e], Pacifico Ruggiero [a]

[a] Dipartimento di Biologia e Chimica Agroforestale ed Ambientale, University of Bari, Via Amendola 165/A, 70126 Bari, Italy
[b] Department of Analytical Chemistry, Ghent University, Krijgslaan 281 S12, B-9000 Ghent, Belgium
[c] Istituto di Metodologie per l'Analisi Ambientale, I.M.A.A., C.N.R., Contrada S. Loja, I-85050 Tito Scalo (PZ), Italy
[d] Department of Chemistry, University of Antwerp, Universiteitsplein 1, B-2610 Wilrijk, Belgium
[e] Karlsruhe Institute of Technology, Institute for Synchrotron Radiation, P.O. Box 3640, D-76021 Karlsruhe, Germany
[f] Karlsruhe Institute of Technology, Institut für Nukleare Entsorgung, P.O. Box 3640, D-76021 Karlsruhe, Germany

Direct mercury (Hg) speciation in chlor-alkali plant contaminated soils enabled the identification of potentially dangerous Hg–S/Cl amorphous species.

ARTICLE INFO

Article history:
Received 28 November 2009
Received in revised form
17 March 2010
Accepted 25 April 2010

Keywords:
Mercury
Soil pollution
Chlor-alkali
Synchrotron
X-rays microanalyses
K106

ABSTRACT

Direct mercury (Hg) speciation was assessed for soil samples with a Hg concentration ranging from 7 up to 240 mg kg^{-1}. Hg chemical forms were identified and quantified by sequential extractions and bulk- and micro-analytical techniques exploiting synchrotron generated X-rays. In particular, micro-spectroscopic techniques such as μ-XRF, μ-XRD and μ-XANES were necessary to solve bulk Hg speciation, in both soil fractions <2 mm and <2 μm. The main Hg-species found in the soil samples were meta-cinnabar (β-HgS), cinnabar (α-HgS), corderoite ($Hg_3S_2Cl_2$), and an amorphous phase containing Hg bound to chlorine and sulfur. The amount of metacinnabar and amorphous phases increased in the fraction <2 μm. No interaction among Hg-species and soil components was observed. All the observed Hg-species originated from the slow weathering of an inert Hg-containing waste material (K106, U.S. EPA) dumped in the area several years ago, which is changing into a relatively more dangerous source of pollution.

1. Introduction

Mercury (Hg) is a toxic element, which can be released into the environment by natural and anthropogenic sources. Hg exists in the environment in a large number of physical and chemical forms, with varying properties that determine its complex distribution, chemical behaviour, biological enrichment and toxicity. Among the various environmental compartments, soil may act as a sink for Hg atmospheric depositions, infiltration of polluted waters, disposal of Hg-contaminated wastes, etc. Therefore special attention should be devoted to the study of this element in soil. To correctly assess and predict Hg mobility and bioavailability in soil, it is necessary to determine its speciation, i.e. to identify and quantify its specific chemical and physical forms in the soil matrix.

Recent, detailed and reliable speciation in soils and sediments for a large number of trace elements has been determined by combining sequential extractions with direct analytical methods exploiting high intensity synchrotron generated X-rays, both at the bulk and micro-scale (Scheinost et al., 2002; Kirpichtchikova et al., 2006; Terzano et al., 2007; Oram et al., 2008; Singer et al., 2009). In particular, highly comprehensive Hg speciation investigations have been carried out by Bernaus et al. (2005a) in polluted soils and in mine environments (Bernaus et al. 2005b, 2006a). The same authors carried out an Hg speciation study on soils in the Netherlands polluted by chlor-alkali plant activities, identifying mainly cinnabar, corderoite, and small quantities of $HgSO_4$ and HgO (Bernaus et al., 2006b).

Chlor-alkali production is one of the main sources of mercury pollution throughout the world (USEPA, 1997). For this reason, different studies have been carried out since several years to assess the impact of chlor-alkali plants on the environment (e.g., Lodenius and Tulisalo, 1984; Maserti and Ferrara, 1991; Biester et al., 2002a,b; Neculita et al., 2005; Zagury et al., 2006; Ullrich et al., 2007).

* Corresponding author.
E-mail address: r.terzano@agr.uniba.it (R. Terzano).

0269-7491/$ – see front matter © 2010 Elsevier Ltd. All rights reserved.
doi:10.1016/j.envpol.2010.04.016

In this paper, we present Hg speciation in Hg-polluted soils collected nearby an industrial area in the South of Italy obtained from bulk Hg-XAS (X-ray Absorption Spectroscopy) results, μ-XRF (micro X-ray Fluorescence spectroscopy), μ-XRD (micro X-ray Diffraction) and μ-XANES (micro X-ray Absorption Near Edge Structure spectroscopy) data, as well as sequential chemical extractions.

Mercury is an "environmentally complex" element which is very difficult to study even with synchrotron techniques, for this reason micro X-ray analyses with synchrotron radiation were necessary to interpret the bulk data.

With such an experimental approach, it has been possible to identify for the first time new forms of potentially more mobile amorphous mercury sulfides.

2. Materials and methods

2.1. Investigated site

The study was conducted in an area of the *Val Basento* industrial site, located near Ferrandina in the district area of Matera, in the South of Italy. This site is included in an Italian National Plan of Environmental Restoration because a large number of industrial activities during the last 40–50 years have caused a diffuse pollution in the area. Further details about the investigated site can be found in Terzano et al. (2007) and Santoro et al. (2010).

2.2. Soil sampling and preparation

Three representative soil samples designated L1, T1, and S5 characterized by different degrees of contamination (Table 1) were investigated. The samples originated from a larger sampling campaign described in Santoro et al. (2010). Sample L1 was collected inside a restricted industrial site, T1 outside the northern part of the restricted industrial site and S5 outside of the southern part. Two composite samples were collected from points T1 and S5, one at 0–10 cm and one at 40–50 cm. For site L1, only one composite sample was collected at 0–10 cm, owing to the shallowness of the soil profile. All the soil samples were homogenized, air dried, sieved at 2 mm, stored in HDPE vessels, and kept at 4 °C prior to analysis. The clay soil fraction (<2 μm) was separated by mixing an amount of 3.5 g of each soil sample with 50 ml of deionized water and stirring for 10 min. Then, the solution was sonicated for 10 min at 100 W by means of a Sonics Vibra-Cell (Sonics and Materials Inc., USA) to mechanically break the soil aggregates. No chemical treatment was used in order to avoid modifications in Hg speciation. After sonication, the suspension was centrifuged for 2.07 min at 600 rpm by using a Mod. CR15-B. Braun Biotech International (USA) centrifuge. The surnatant containing the clay fraction was collected and centrifuged at 5500 rpm for 30 min. The final solid residue was then lyophilized using a Hetosicc (Hetolab equipment, Denmark) lyophilizer and stored at 4 °C for further analysis. Finally, the dimension of the particles was verified by scanning electron microscope (SUPRA40, Carl Zeiss).

2.3. Total mercury determination

The total mercury concentration in the soil samples was determined using an Automatic Mercury Analyzer (AMA 254, FKV, Altec). This instrument allowed the direct Hg determination in soil samples without sample chemical pre-treatment such as total acidic dissolution, alkaline fusion, etc. (Santoro et al., 2010).

2.4. Sequential extractions

A seven step sequential extraction procedure (SEP) already employed to study Hg in soils and mine environments (Bernaus et al., 2006b; Quejido et al., 2002; Sánchez et al., 2005) was used to determine the partitioning of Hg associated with different soil constituents and to elucidate the potential availability and mobility of Hg according to the solubilization promoted by various extracting solutions.

The extracted fractions can be briefly described as follows: F1) Water-soluble fraction (0.5 g soil + 25 ml deionized water; 1 h): Hg weakly bound to the soil matrix, that can be easily released, thus becoming immediately available following a simple leaching by rainwater; F2) Exchangeable (Residue + 8 ml NH_4Cl 1 M, pH 7; 1 h): Hg electrostatically bound to clay surfaces, hydrated oxides of iron and manganese and humic substances; F3) Carbonates (Residue + 20 ml CH_3COONH_4 1 M, pH 4.5; 4 h): Hg bound to carbonates; F4) Easily reducible (Residue + 20 ml Tamm's solution; 4 h): Hg bound to amorphous Fe/Mn (hydr)oxides; F5) 6 M HCl soluble (Residue + 30 ml HCl 6 M; 2 h): Hg bound to crystalline Fe-(hydr)oxides, crystalline Al and Mn oxides, elemental Hg, Hg_2Cl_2, metacinnabar; F6) Oxidizable (Residue + 5 ml H_2O_2 8.8 M, pH 2, 2 h; then Residue + 25 ml CH_3COONH_4 1 M, pH 2, 16 h): Hg bound to organic matter; F7) Residue (directly analyzed by AMA 254): Hg strongly bound to soil matrix in primary and secondary minerals or as highly insoluble compounds (e.g., cinnabar).

Total mercury concentration in each extracted fraction was determined by using an Automatic Mercury Analyzer (AMA 254, FKV, Altec) (Sánchez et al., 2005).

2.5. XAS analyses

Bulk XAS data were acquired at the XAS (X-ray Absorption Spectroscopy) beamline and INE-Beamline (Institut für Nukleare Entsorgung) for actinide research at the ANKA synchrotron facility (Karlsruhe, Germany), a 2.5 GeV electron storage ring.

Soil samples and Hg-standards (see Section 2.6) were measured as fine powders pressed into 13 mm diameter pellets. When necessary, samples and standards were properly diluted with boron nitride (Sigma–Aldrich).

Data were recorded both at room temperature and at 15 K (He-cryostat) from 12134 eV to 12836 eV (around the Hg-L_{III} absorption edge at 12284 eV) in fluorescence or in transmission mode for soil samples and Hg-standards, respectively. A Si (111) crystal pair was used in the monochromator for all the measurements. The energy was initially calibrated against the first inflection point of a gold foil (Au-L_{III} 11919 eV). Thereafter, an $HgCl_2$ standard was regularly measured during the experiment, to correct any energy displacement (Bernaus et al., 2005a). Three scans were averaged for the XAS spectra of the Hg-standards, five to eight scans for the soil samples.

The XAS data reduction was accomplished by using the IFEFFIT software package (1.2.11 version), containing *Athena*, *Artemis* and *Sixpack* softwares (Ravel and Newville, 2005; Webb, 2005), and WinXAS (Ressler, 1998).

A combination of principal component analysis (PCA), target transformation, and linear combination least-squares fitting (LCF) of Hg-L_{III} edge soil samples spectra with the spectra of known Hg-standard compounds was used for XANES spectra analysis.

The quality of the fit was estimated by calculating the residual $R = [\Sigma\,|y_{exp}\,(i) - y_{fit}\,(i)|/\Sigma\,|y_{exp}\,(i)|] \times 100$ (Ressler et al., 2000). A lower R value represents a better match between the fitted model spectra and the experimental spectrum.

2.6. Hg-reference compounds

The following Hg-standards have been analyzed for comparison with the spectra of unknown samples: elemental Hg, cinnabar (α-HgS), metacinnabar (β-HgS), HgO, $HgCl_2$, Hg_2Cl_2, $HgSO_4$, Hg_2SO_4, $Hg(CH_3COO)_2$, corderoite ($Hg_3S_2Cl_2$), Kleinite ($Hg_2N(Cl,SO_4)\cdot nH_2O$), Eglestonite ($Hg_6Cl_3O_2H$), Terlinguaite ($Hg_4O_2Cl_2$), Hg(II) complexed by humic acids (Hg-HA), Hg(II) sorbed to goethite (Hg–goethite) and K106, a synthetic reference sludge.

Pure Hg compounds were purchased from Sigma–Aldrich, eglestonite and terlinguaite were provided by the "Museum of Earth Sciences–Department of Geology" (University of Bari, Italy), while corderoite (Mcdermitt, Nevada), kleinite (Mcdermitt, Nevada) and vrbaite (Lookout Pass, Utah) were purchased from Minerals and More® (USA).

Hg-HA was prepared according to the following procedure: 60 mg humic acid (EUROSOIL E5; Senesi et al., 2003) were suspended in 100 ml 0.05 mM $Hg(NO_3)_2$ solution at pH 4 (HNO_3), stirred for 24 h, centrifuged, washed with deionized water and lyophilized to recover the final Hg-HA complex.

The Hg–goethite standard was prepared according to Bonnissel-Gissinger et al. (1999): 400 mg of pure goethite (Bayferrox 910-standard 86, Bayer) were mixed with 35 ml of 0.1 M NaCl solution. Five milliliters of a $Hg(NO_3)_2$ solution (25 mg kg^{-1} in Hg^{2+}) were added to the mixture and the final pH was regulated to 8.5 by adding 0.1 M NaOH. The solution was then stirred for 72 h. After centrifugation, the Hg–goethite complex formed was repeatedly washed with deionized water and then lyophilized.

K106 is a mercury-bearing sludge resulting from the treatment of effluents from the electrolytic process employed to generate chlorine gas and sodium hydroxide in chlor-alkali plants, and consists principally of mercuric sulfides. The K106 sludge is an U.S. EPA (Environmental Protection Agency) Resource Conservation and Recovery Act (RCRA)-listed waste characterized by a typical composition (Sass et al., 1994). As reported by Dungan (1992), the K106 composition range is: mercury (1–12%), sulfur (0.4–15%), inorganic salts (mainly NaCl: 3–15%), water (24–58%). K106 waste sludge was synthesized according to the procedures adopted in the chlor-alkali plants during the 1980's (Hagemoen et al., 1994). In particular, two different procedures were employed: i) Elemental mercury Hg^0 (12 g) was mixed with a solution containing 10 ml NaClO (8% in chlorine), 3 ml of HCl (36%) and 10 g of NaCl and stirred overnight. Then, 113 g of $Na_2S^*9H_2O$ were added and the mixture was left to react an additional night. The pH of the solution was kept at 3 by adding HCl (36%). The solution was then aged in a closed vessel exposed to sunlight for 10 days. The final suspension was evaporated to dryness in an aerated oven at 30 °C; ii) elemental mercury Hg^0 (12 g) was transformed to HgS by adding α-S (15 g) in a NaCl (15 g) solution (58 ml deionized water) and stirred for 24 h at room temperature. The pH of the solution was kept at 3 by adding HCl (36%). The solution was aged in sunlight for 10 days and finally evaporated to dryness at 30 °C in an aerated oven.

The synthesis products were analyzed by XANES spectroscopy and the spectra for both the synthesized K106 products were essentially the same, suggesting an

almost identical composition, at least for the Hg-bearing phases. Therefore, only one of them was additionally characterized by quantitative XRD (see Section 2.8).

2.7. Synchrotron microprobe analyses

Microprobe analyses (μ-XRF, μ-XRD, and μ-XANES) were performed at HASYLAB Beamline L (DESY, Hamburg, Germany) and at SUL-X beamline (ANKA, Karlsruhe, Germany). HASYLAB operates at positron energy of 4.5 GeV. Additional details about the experimental set-up and operation for combined microprobe analyses can be found in Terzano et al. (2007).

For the micro-analytical studies, thin sections were prepared from soil samples sieved at 2 mm, air dried and embedded in acrylic resin (L.R. White, SPI Supplies). Resin polymerization was carried out at room temperature by using an Hg-free catalyst (SPI Supplies). Solid soil blocks embedded in resin were obtained following air-drying and polishing with silicone carbide with decreasing grain size. Subsequently, the blocks were cut, glued on ultrapure fused quartz slides (900 μm thick, SPI) using an epoxy resin (Araldite 2020/A), and polished into thin sections of 30 μm. A total of three thin sections for each of the samples L1, T1 and S5 were prepared from three different blocks and analyzed. Various areas of the soil thin sections ranging from 400 μm^2 up to few mm^2 were scanned while collecting μ-XRF data with a beam size of 20 μm^2. In this way, Hg-rich spots or areas could be identified for subsequent μ-XANES and μ-XRD measurement.

The μ-XRF data were evaluated using the *Axil* (Vekemans et al., 1994) and *PyMca* (Solé et al., 2007) programs. The μ-XRD diffraction images and diffractograms were processed using *Fit-2D* (Hammersley, 2004) and *XRDUA* (De Nolf, 2006) software packages. The μ-XANES spectra were analyzed using WinXAS (Ressler, 1998).

2.8. K106: XRD characterization

An XRD pattern was collected for the K106 synthesis product ii) (see Section 2.6) using a Rigaku D-Max Rapid micro-diffractometer operating at 40 kV and 30 mA with Cu-K_α radiation and flat graphite monochromator. The quantitative analysis was obtained by Rietveld refinement, using the EXPGUI software (Toby, 2001), after XRD powder data collection with high crystalline corundum NIST 676 as internal standard.

3. Results and discussion

3.1. Soil characteristics and Hg content

Selected physical and chemical characteristics of the investigated soils are summarised in Table 1. All the soils are characterized by an alkaline pH, ranging from 8.0 to 8.5. L1 and S5 are loam soils, while T1 is sandy loam (USDA). S5, L1 and $T1_{40-50}$ samples have a low organic carbon content (C_{org}), from 0.6 to 1.4%, while $T1_{0-10}$ shows a three times higher C_{org} content of about 3%. The amount of Fe_2O_3 on the average is ca. 5.0% for all the soil samples. The three samples L1, T1 and S5 show different degrees of Hg contamination. The total Hg concentration in L1 is about 240 mg kg^{-1}; in S5 it ranges from 7.3 mg kg^{-1} (0–10 cm) to 12 mg kg^{-1} (40–50 cm) and from 50 mg kg^{-1} (0–10 cm) to 9.2 mg kg^{-1} (40–50 cm) in T1. Interestingly, Hg is highly concentrated in the clay fraction (<2 μm), especially for samples $S5_{40-50}$ and $T1_{0-10}$ where Hg is 2.5 times more concentrated than in the <2 mm fraction. This aspect is relevant for these samples, as their clay fraction accounts for about 20% in weight and it is well known that clay particles, especially the nanometer-sized ones, can potentially be mobilized in soil as colloidal dispersions in water fluxes or in the atmosphere as airborne particles.

The results of the seven steps SEP are shown in Table 1. The mercury (80–90%) could be extracted only by using concentrated acids (6 M HCl: F5) or remained in the residual fraction (RES). Only in sample $T1_{0-10}$, the sample with the highest C_{org} content, a small percentage of Hg (3%) in the oxidizable fraction (F6) was observed. Essentially no mercury was recovered in the more labile SEP fractions (F1–F4: water soluble, exchangeable, weak acidic conditions and complexing agents).

3.2. Bulk and micro-XAS analyses

Bulk XAS spectra were collected for the samples with the highest Hg content: both <2 mm and <2 μm fractions of L1, $S5_{40-50}$ and $T1_{0-10}$. Spectra were collected either at room temperature or at 15 K. No difference was observed between the spectra acquired at the two temperatures, therefore only the data acquired at room temperature are shown here. The EXAFS part of the acquired spectra was not used for the soil samples because of the high noise level registered.

The analyzed soil samples showed very similar bulk XANES spectra (Fig. 1b and c).

From PCA results, two components were found sufficient to reconstruct all the sample spectra. To assess which standards were good candidates to be used in LCF, a SPOIL value was determined for the various Hg-reference compounds (Malinowski, 1978; Webb, 2005). Eight standards gave a SPOIL value below 4.5 (good for 1.5–3; fair for 3–4.5; poor for 4.5–6) and were therefore used in LCF: K106 (2.2), β-HgS (2.7), Hg–goethite (3.2), $HgCl_2$ (3.4), corderoite (3.7), α-HgS (3.9), HgO (4.3), Hg^0 (4.4).

Despite these indications, it was not possible to perform satisfactory LCF in the XANES region by simply using the Hg-standard compound spectra to model any of the sample data. In all cases, the modeled XANES profiles were so different from the experimental ones that no reliable assumption on Hg speciation could be done. Therefore, the soil samples were investigated with a microfocussed beam to attain spatially resolved XANES information. μ-XANES spectra were collected from various Hg-rich locations identified by means of elemental mapping (see Section 3.3) for all the investigated samples. Interestingly, all the Hg-rich spots that were analyzed exhibited essentially two main types of μ-XANES spectra (B1 and B2; Fig. 1a). All bulk XANES spectra collected for the soil samples L1, $T1_{0-10}$ and $S5_{40-50}$, for both <2 mm (Fig. 1b) and <2 μm (Fig. 1c) fractions could satisfactorily be described by a LCF of these two μ-XANES spectra.

3.3. Combined X-ray microprobe analyses

Evaluation of the μ-XRF spectra collected on the Hg-rich spots showed the co-presence of Cl and S with the Hg. The presence of S and Cl was better evidenced by acquiring the spectra at a low excitation energy (3 keV) and in vacuum. Analysis of the correlation between elements showed that, in general, there was a linear correlation between Hg and Cl, and Hg and S, but not between Hg and Fe (Fig. 2). This indicates an association of Hg with Cl and S and that it is not bound to Fe-bearing minerals [e.g., Fe (hydr)oxides], as often observed for Hg. The association of Hg with amorphous or low-crystalline Fe (hydr)oxides could be already excluded from the

Table 1
Soil samples characteristics, Hg total content and Hg distribution in different extractable fractions. F# subscripts refer to the relative fraction of Hg associated with the seven step (steps 1 through 6 and residual, RES) sequential extraction procedure.

Soil Sample	pH	C_{org} (% d.w.)	<2 μm (% d.w.)	Hg_{Tot} (mg kg^{-1})	$Hg_{<2\ \mu m}$ (mg kg^{-1})	Hg_{F1-F4} (%Hg_{Tot})	Hg_{F5} (%Hg_{Tot})	Hg_{F6} (%Hg_{Tot})	Hg_{RES} (%Hg_{Tot})
L1	8.5	1.40	13	240 ± 40	203 ± 13	0	85	0	15
$S5_{0-10}$	8.2	0.62	23	7.3 ± 0.6	12.9 ± 0.4	0	90	0	10
$S5_{40-50}$	8.5	0.68	21	12.1 ± 1.7	30 ± 2	0	90	0	10
$T1_{0-10}$	8.0	2.98	16	50 ± 5	135 ± 14	0	87	3	10
$T1_{40-50}$	8.4	0.83	17	9.2 ± 0.7	14.2 ± 0.3	0	84	0	16

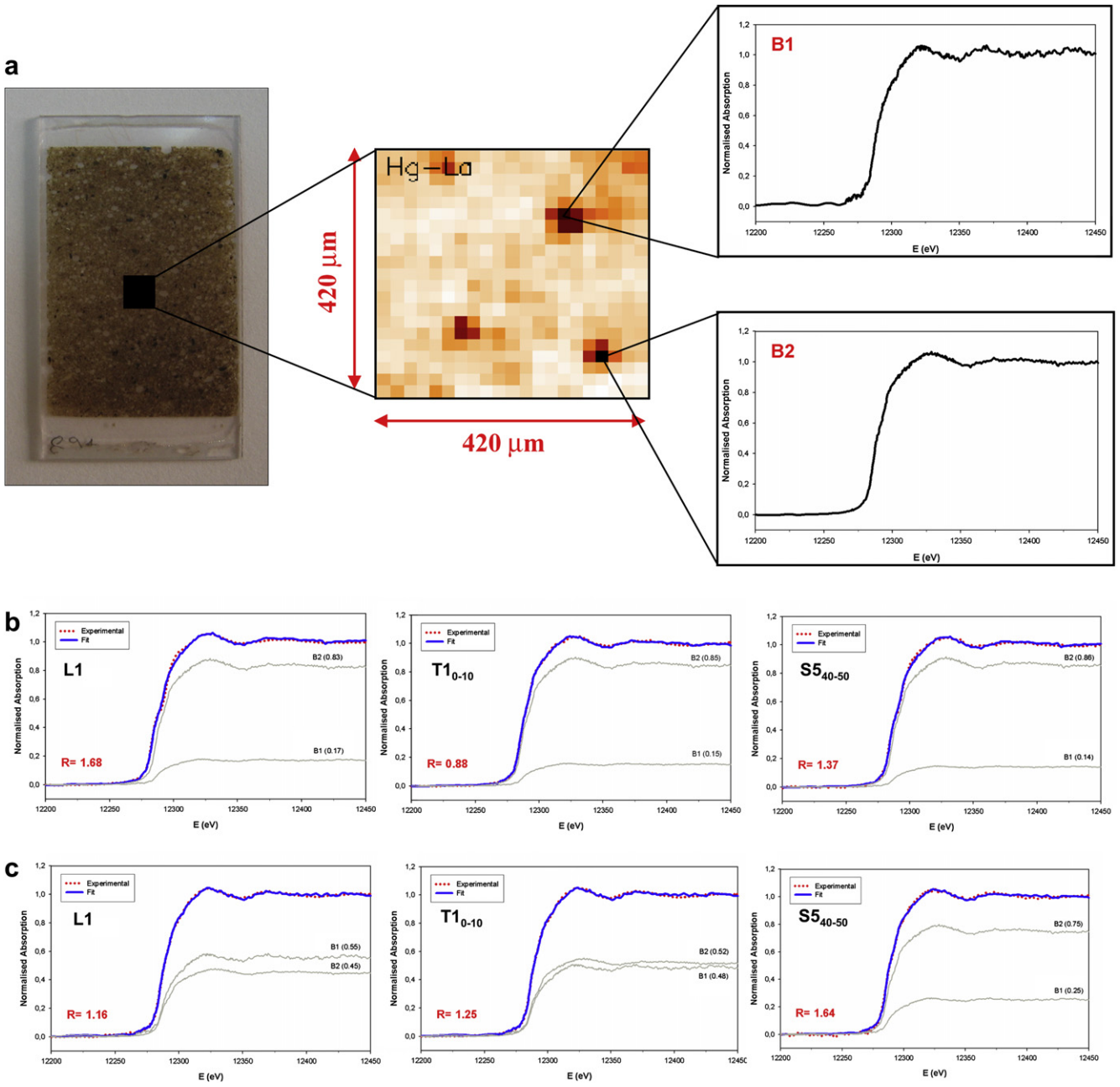

Fig. 1. μ-XANES spectra (B1 and B2) collected at Hg-rich spots in the analyzed thin sections (a). Linear combination fitting for samples L1, $T1_{0-10}$ and $S5_{40-50}$ for the <2 mm (b) and <2 μm (c) fractions, using spectra B1 and B2 as reference compound spectra. The fractional contribution of the principal components making up the fitted spectra also is reported together with the evaluation parameter of the fit (*R*).

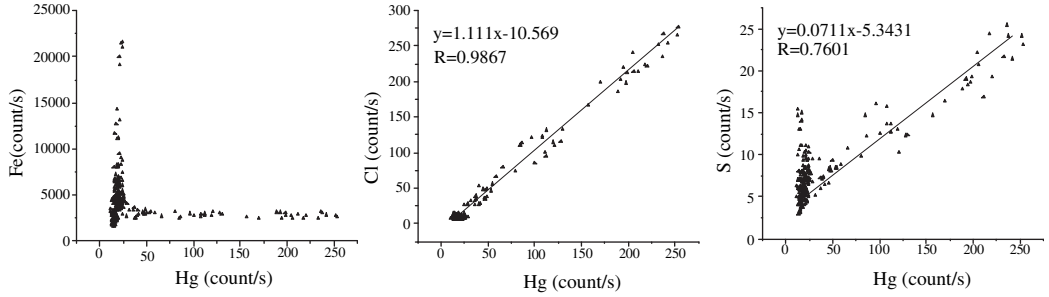

Fig. 2. Scatterplots (or pair correlation diagrams) obtained from a μ-XRF map of sample $T1_{0-10}$ (average of 5 regions containing Hg-rich particles). The measured Hg Lα versus Fe, Cl and S Kα fluorescence intensities are represented in count s^{-1}. Similar trends were observed also for sample L1 and $S5_{40-50}$.

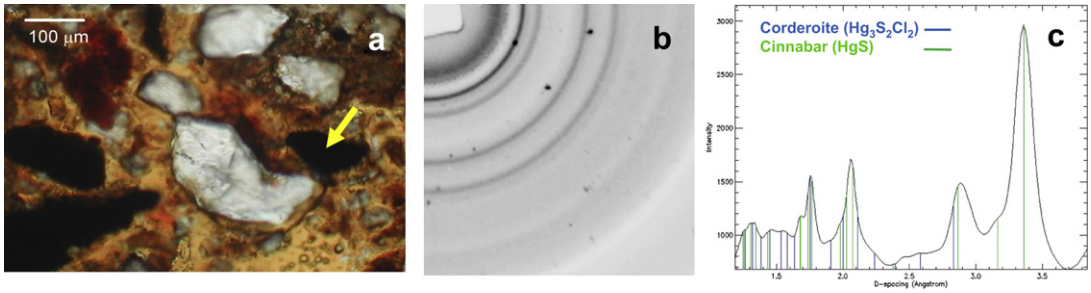

Fig. 3. Transmitted optical image of a microscopic area on L1 soil thin section analyzed by μ-XRD (a). μ-XRD image (b) collected for the black Hg-rich particle indicated by the yellow arrow in (a). The corresponding diffraction pattern is reported (c). The characteristic d-spacings for cinnabar (green line) and corderoite (blue line) are also shown. (For interpretation of the references to colour in this figure legend, the reader is referred to the web version of this article).

results of the SEP. These data suggest that Hg is also not associated to crystalline Fe (hydr)oxides. The Hg is more likely to be present as a scarcely soluble chemical form containing S and Cl.

μ-XRD analyses did not show significant diffraction patterns for the Hg-rich areas directly attributable to crystalline Hg-species. This indicates that either Hg is present in amorphous forms or that the diffracting volume of the Hg-containing particles is too small to give rise to diffraction patterns of sufficient intensity. A detectable diffraction pattern could be obtained only from the larger Hg-containing particles (ca. 100 μm) observed in sample L1 (Fig. 3a). The diffractograms suggested the co-presence of two Hg-minerals in these particles: cinnabar and corderoite (Fig. 3b,c).

The presence of Hg–Cl, Hg–S and Hg–Cl–S compounds (including mercuric chloride, cinnabar, metacinnabar and corderoite) in Hg-containing soils and sediments has been frequently reported in the literature (Revis et al., 1989; Barnett et al., 1997; USEPA, 1997, 2007; Kim et al., 2000). In the presence of a significant amount of organic matter, Hg can also be found as HgO or bound to humic acids (Andrews, 2006). The affinity of Hg for organic matter and especially for S-containing groups of organic molecules is well known (Xia et al., 1999; Yue et al., 2006). However, in our samples, sequential extraction studies seem to exclude any significant amount of Hg bound to organic matter.

The B1 and B2 μ-XANES spectra, used to fit the bulk XANES spectra for all the investigated soil samples (Fig. 1), were then interpreted by using a LCF of selected standards chosen following the PCA (Section 3.2) and the information obtained from the microanalyses. The B1 XANES nearly matches exactly the K106 spectrum (Fig. 4a). The best fit for B2 was obtained with 40% corderoite, 28% K106, and 32% cinnabar (Fig. 4b).

3.4. K106: EXAFS and XRD characterization

K106 is generically said to contain mercuric sulfides (Twidwell and Thompson, 2001) but, to our knowledge, no detailed characterization was ever performed. Therefore, we characterized our K106 reference compound by using EXAFS and quantitative X-ray diffraction.

The EXAFS spectrum and the corresponding Fourier transform for K106 are reported in Fig. 5. The EXAFS data, analyzed using theoretical scattering and phase functions (Ravel, 2007; Wyckoff, 1963), revealed the presence only of Cl and S atoms in the 1st shell (Hg–Cl = 2.5 ± 0.1 Å with a coordination number-CN = 4.1; Hg–S = 2.5 ± 0.3 Å, CN = 2.2) and of Cl and Hg in the 2nd shell (Hg–Cl = 3.2 ± 0.3 Å, CN = 0.4; Hg–Hg = 4.1 ± 0.4 Å, CN = 2).

The Hg–S and the Hg–Cl distances found in the 1st shell and the Hg–Hg and Hg–Cl in the 2nd shell are similar to the bond lengths in metacinnabar (Hg–S: 2.53 Å; Hg–Hg: 4.13 Å) and Hg_2Cl_2 (Hg–Cl: 2.52 Å and 3.19 Å) (Wyckoff, 1963).

The Hg–S distances in the 1st shell and the Hg–Cl distances in the 2nd shell are also very similar to those in corderoite structure (Hg–S: 2.45 Å, Hg–Cl: 3.38 Å, Frueh and Grey, 1968; Foord et al., 1974). The Hg–Hg distances typical for metallic mercury (Hg^0, Hg–Hg = 2.99 Å and 3.46 Å) were not observed, neither at 15 K.

Nevertheless, in this study the atomic distances and especially the coordination numbers obtained could not be directly ascribed to one of these specific crystalline Hg-containing minerals. For instance, the Hg–S distance (2.53 Å) in the metacinnabar structure exhibit a CN = 4 and Hg–Hg (4.13 Å) CN = 12; whereas Hg–Cl bonds (2.52 Å and 3.19 Å) in Hg_2Cl_2 structure show CN = 1 and 4, respectively (Wyckoff, 1963). Only the CN of Hg–S bonds in the 1st shell present a value comparable to those found in metacinnabar and in corderoite.

These data may suggest that Hg i) is present in a number of Hg-mineral phases leading to an average structure unlike any known phase, ii) is present without a well-defined structure, i.e. in an amorphous state, or iii) is present as an unknown mineral.

Rietveld analysis of the XRD data (Fig. 6) shows the synthesized K106 to contain the following phases: 20% metacinnabar (β-HgS),

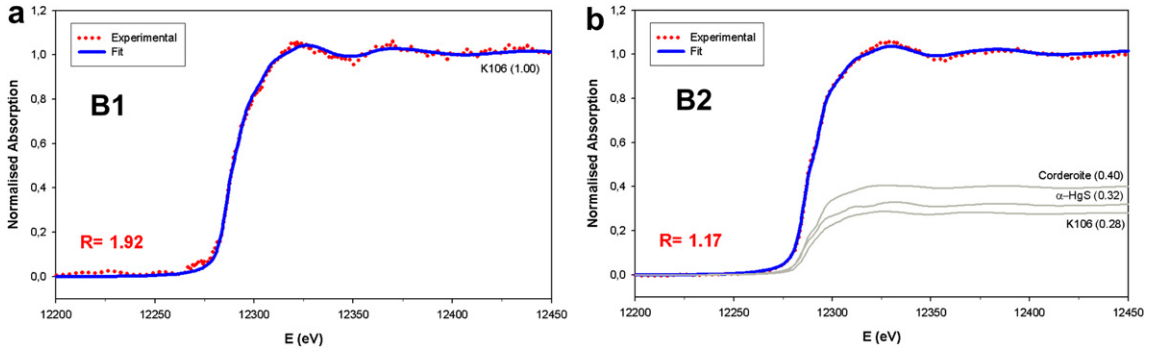

Fig. 4. Linear combination fit results for B1 (a) and B2 (b) spectra achieved including synthetic K106 as a reference compound.

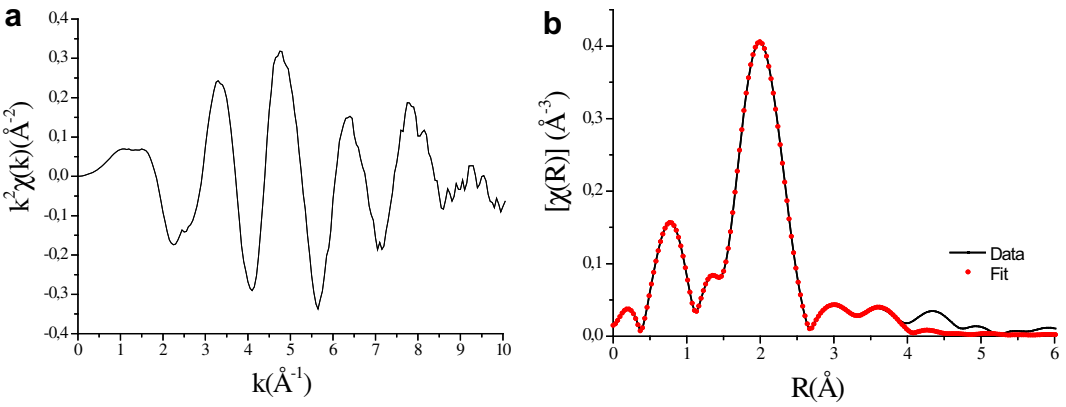

Fig. 5. EXAFS spectrum of K106 (a) and corresponding Fourier transform and fit (red points) (b). Fitting range: 1–4.0 Å. (For interpretation of the references to colour in this figure legend, the reader is referred to the web version of this article).

20% halite (NaCl), 26% α-S and 34% of an amorphous phase. The presence of metacinnabar was also suggested by the EXAFS data. As the reagents employed in the synthesis of K106 are all crystalline S or Cl containing phases (with the exception of Hg^0, whose presence is already excluded by the EXAFS data), we can assume, also on the basis of the EXAFS investigation, that the amorphous phase, accounting for the highest percentage constituent of the K106, is most likely an amorphous species containing Hg bound to S and Cl.

3.5. Final Hg speciation and environmental implications

We could derive the final mercury speciation in our soil samples for the <2 mm and the <2 μm fractions (Table 2, Column C) by considering the LCF results to the bulk XANES spectra using a combination of B1 and B2 μ-XANES spectra (Fig. 1b,c and Table 2, Column A). As it is reported in Fig. 4, B1 can be fit by K106 (100%) while B2 by a combination of cinnabar (32%), corderoite (40%) and K106 (28%). Therefore, as a first approximation, Hg speciation in the soil samples can be expressed in terms of these three standards as reported in Table 2, Column B. Finally, by considering that XRD data on K106 (Section 3.4) suggested that with regard to Hg compounds this material is most likely composed of metacinnabar (37%) and amorphous Hg phases containing S and Cl (63%), the contribution of K106 can be explicated in terms of these two phases thus leading to the final Hg speciation reported in Table 2, Column C.

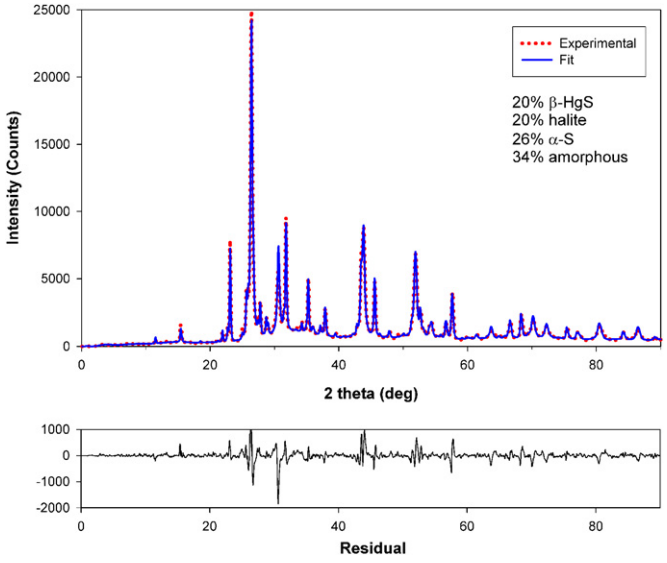

Fig. 6. Results of the quantitative analysis performed for the synthesized K106 product by using XRD powder diffraction and Rietveld refinement. The internal standard used was corundum NIST 676. The red points represent the experimental data, while the blu line is the reconstructed diffraction pattern. The residual is shown at the bottom. (For interpretation of the references to colour in this figure legend, the reader is referred to the web version of this article).

It must be pointed out that the contribution of the amorphous phase to Hg speciation could have been overestimated owing to the indirect method employed to extrapolate its contribution (Section 3.4). In general, the accuracy of the LCF technique adopted is of the order of ca. 20% and Hg-containing phases below 10% are not statistically significant (Kim et al., 2000).

The presence of relevant concentrations of HgS (both as cinnabar and metacinnabar) could explain the high amount of Hg found in the F5 and RES SEP fractions (Table 1). Usually, HgS is associated with the residual fraction (Sánchez et al., 2005). However, Mikac et al. (2002) established that 6 M HCl can also extract both metacinnabar and cinnabar, with metacinnabar showing a higher tendency to be dissolved in this step. The same authors also found that poorly crystalline metacinnabar synthesized in the laboratory seemed to be redissolved more readily under high acidic conditions than the corresponding crystalline forms. Therefore, metacinnabar, especially the poorly crystalline one, may have been preferentially dissolved in our F5 fraction rather than remaining in the residual (RES). The residual could, in turn, account for highly crystalline cinnabar. Similar results were obtained by Kim et al. (2003) for a marine sediment. In particular, they ascribed the higher solubility of metacinnabar in the sediment sample to the nanometer size of the metacinnabar particles. Nevertheless, dissolution of metacinnabar alone cannot explain the large amount of Hg dissolved in the F5 step (ca. 80%). On the basis of our data, it is reasonable to conclude that other insoluble species such as corderoite and amorphous phases containing Hg, S and Cl could also have been extracted in this step. It is known that chemical species containing S and Cl bound to Hg, are characterized by a relatively higher solubility than HgS (Paquette and Helz, 1995).

It is interesting to note that the amorphous Hg-bearing phases account for a very high percentage in all the samples, especially in the <2 μm fraction (Table 2, Column C). In addition, in the fraction <2 μm the amount of amorphous phases and metacinnabar is significantly higher and the amount of cinnabar and corderoite lower in comparison to that of the <2 mm fraction.

Lowry et al. (2004), in trying to explain the discrepancies between the results of sequential extractions and EXAFS observed in colloids generated from New Idria mercury mine tailings, beside invoking the

Table 2
Percentage results of the LCF for the <2 mm and <2 μm fractions of the soil samples L1, $T1_{0-10}$ and $S5_{40-50}$, achieved by using A) B1 and B2 μ-XANES spectra (Fig. 1); B) the results of the fitting of B1 and B2 (Fig. 4); C) the results of the fitting of B1 and B2, and the composition of K106 (37% metacinnabar, 63% amorphous), as determined by XRD (only Hg-containing phases).

Sample (<2 mm)	A		B			C			
	B1	B2	Cinnabar (α-HgS)	Corderoite ($Hg_3S_2Cl_2$)	K106	Cinnabar (α-HgS)	Metacinnabar (β-HgS)	Corderoite ($Hg_3S_2Cl_2$)	Amorphous (Hg, S, Cl)
L1	17	83	27	33	40	27	15	33	25
$T1_{0-10}$	15	85	27	34	39	27	14	34	25
$S5_{40-50}$	14	86	28	34	38	28	14	34	24
Sample (<2 μm)									
L1	55	45	14	18	68	14	25	18	43
$T1_{0-10}$	48	52	15	21	64	15	23	21	41
$S5_{40-50}$	25	75	24	30	46	24	18	30	28

small size of the Hg-containing particles (<100 nm) also hypothesized the presence of an unidentified Hg-containing phase in the sample. In their study, they supposed this phase to be elemental Hg. However, as observed by Slowey et al. (2005), over time elemental Hg is transformed into other species such as soluble oxides and chlorides, organically bound and adsorbed Hg, as well as insoluble Hg–sulphides. In addition, elemental Hg can be easily lost from soil by volatilizing into the atmosphere (Carpi and Lindberg, 1997).

In the chlor-alkali plants using Castner–Kellner technology very large quantities of mercury were handled and a huge volume of Hg-contaminated wastewater was produced. A common practice for treating the contaminated wastewater prior to discharge was to precipitate the mercury in the form of insoluble sulfides. These treatments produced the waste sludge listed as K106 by the U.S. EPA. Until 1992 the common practice was that, once filtered, this waste was land disposed. After this date, new regulations required K106 waste to be thermally treated.

The sulfide precipitate produced during operation of chlor-alkali plants was very fine and typically under 5 μm (USEPA, 2007). This could explain the highest contribution of the Hg constituents found to be associated with the synthetic K106 (amorphous phases and metacinnabar) in the soil fraction <2 μm.

According to our data, the synthetically prepared K106 contains metacinnabar. However, the most thermodynamically stable HgS form in the environment is generally cinnabar. In addition, we find substantial amounts of corderoite, especially in the <2 mm fraction. This is in agreement with our μ-XRD observations showing these two minerals to be in the largest Hg-containing particles of about 100 μm. It is known (Foord et al., 1974; Spring and Grout, 2002; Cotte et al., 2006) that corderoite can be formed from cinnabar in the presence of chlorine, via a photochemical transformation. We interpret the Hg speciation in the soil samples as indicating that metacinnabar, originally a constituent of K106 chlor-alkali waste, slowly (probably years) converted into cinnabar (the most stable HgS form). The fact that the cinnabar is generally more concentrated in the fraction <2 mm rather than in the clay (<2 μm) fraction and that the μ-XRD diffractogram of cinnabar was only detectable in the larger Hg-containing particles, suggests that the transformation is accompanied by an increase in crystallite size. After formation, the cinnabar is transformed into corderoite: a process that is described in numerous studies. McCormack (2000) has observed that cinnabar, in contact with a saline (NaCl) solution blackens while the solution is evaporated under sunlight. This black product was found to be corderoite (Spring and Grout, 2002). This aspect is responsible for the well-known process called *blackening* of red cinnabar, of high interest in cultural heritage studies (McCormack, 2000). The production of K106 in chlor-alkali plants was carried out in the presence of high concentrations of NaCl (brine solution) and therefore the transformation of cinnabar (red) in contact with a saline (NaCl) solution after light exposure to corderoite (black) is likely. However, considering the limited penetration of sunlight radiating into soil, possibly the photodegradation of cinnabar under sunlight had occurred when the K106 waste was stocked or when the K106 sludge was spread on the soil surface. Anyhow, further investigation to clarify these processes is needed. Note that the highly inhomogeneous mercury distribution observed in the investigated area excludes Hg contamination via atmospheric deposition (Santoro et al., 2010).

4. Conclusions

All the data presented suggest that the observed soil Hg contamination was most probably caused by the dumping of waste material containing a high concentration of mercury (K106) produced by a chlor-alkali plant operating in the area until the 1980s. The Hg speciation observed in the soil samples is interpreted as resulting from an initial formation of fine metacinnabar crystals and amorphous Hg–S/Cl species in the origin of the Hg contamination, i.e. the K106 sludge during a fast crystallization process. Over time, larger cinnabar crystals formed from transformation and agglomeration of smaller metacinnabar grains into cinnabar. Upon exposure to sunlight (the K106 material being spread out over the soil surface) and in the presence of Cl, cinnabar was then partially transformed into corderoite.

In closing we point out that our results also suggest to pay particular attention to the submicrometer-sized soil particles that can potentially pose a serious danger for other environmental compartments, as well as for humans, e.g., by colloidal mobilization in water fluxes or by inhalation. In addition, the effect of chlorine and light on HgS forms, thus producing relatively more soluble species, should be considered when investigating insoluble HgS in chlorine-rich environments (e.g., soils surrounding chlor-alkali plants or marine sediments). This research also demonstrates that, because of the high complexity of soil matrices, no single analytical technique is capable of providing all necessary and desired information for a complete and exhaustive metal speciation. The combined use of direct techniques such as those employing synchrotron generated X-rays, and in particular microbeam investigations, provide very significant advantages, leading to an accurate metal speciation of soil samples, identification of the source of pollution and evaluation of potential associated hazards.

Acknowledgements

This research was partially financed by the MIUR (COFIN 2005) project “Innovative chemical, physical, and biological methods to characterize and remediate soils polluted by heavy metals (MICROS)”. Synchrotron experiments at HASYLAB were financially

supported by the European Community-Research Infrastructure Action under the FP6 "Structuring the European Research Area" Program I(Integrating Activity on Synchrotron and Free Electron Laser Science; project: contract RII3-CT-2004-506008). This research was also performed as part of the "Interuniversity Attraction Poles" (IAP6) Program financed by the Belgian government. We thank Gerald Falkenberg and Karen Rickers-Appel for their scientific and technical support in obtaining the experimental data at Beamline L (HASYLAB, DESY, Hamburg, Germany).

References

Andrews, J.C., 2006. Mercury speciation in the environment using X-ray absorption spectroscopy. Struct. Bond. 120, 1–36.
Barnett, M.O., Harris, L.A., Turner, R.R., Stevenson, R.J., Henson, T.J., Melton, R.C., Hoffman, D.P., 1997. Formation of mercuric sulfide in soil. Environ. Sci. Technol. 31 (11), 3037–3043.
Bernaus, A., Gaona, X., Ivask, A., Karhu, A., Valiente, M., 2005a. Analysis of sorption and bioavailability of different species of mercury on model soil components using XAS techniques and sensor bacteria. Anal. Bioanal. Chem. 382, 1541–1548.
Bernaus, A., Gaona, X., Valiente, M., 2005b. Characterization of Almadén mercury mine environment by XAS techniques. J. Environ. Monit. 7, 771–777.
Bernaus, A., Gaona, X., Esbri, J.M., Higueras, P., Falkenberg, G., Valiente, M., 2006a. Microprobe techniques for speciation analysis and geochemical characterization of mine environments: the mercury district of Almadén in Spain. Environ. Sci. Technol. 40, 4090–4095.
Bernaus, A., Gaona, X., van Ree, D., Valiente, M., 2006b. Determination of mercury in polluted soils surrounding a chlor-alkali plant. Direct speciation by X-ray absorption spectroscopy techniques and preliminary geochemical characterization of the area. Anal. Chim. Acta 565, 73–80.
Biester, H., Müller, G., Schöler, H.F., 2002a. Estimating distribution and retention of mercury in three different soils contaminated by emissions from chlor-alkali plants: part I. Sci. Total Environ. 284, 177–189.
Biester, H., Muller, G., Scholer, H.F., 2002b. Binding and mobility of in soils contaminated by emissions from chlor-alkali plants. Sci. Total Environ. 284, 191–203.
Bonnissel-Gissinger, P., Alnot, M., Lickens, J.-P., Ehrhardt, J.-J., Behra, P., 1999. Modeling the adsorption of mercury (II) on (hydr)oxides II: α-FeOOH (Goethite) and amorphous silica. J. Colloid Interface Sci. 215, 313–322.
Carpi, A., Lindberg, S.E., 1997. Sunlight-mediated emission of elemental mercury from soil amended with municipal sewage sludge. Environ. Sci. Technol. 31, 2085–2091.
Cotte, M., Susini, J., Metrich, N., Moscato, A., Gratziu, C., Bertagnini, A., Pagnao, M., 2006. Blackening of Pompeian cinnabar paintings: X-ray microscopy analysis. Anal. Chem. 78, 7484–7492.
De Nolf, W., 2006. XRDUA Version 3.3.1.9 Available at. http://xrdua.ua.ac.be/ Available at Last accessed 11 2009.
Dungan, A.E., 1992. Development of BDAT for the thermal treatment of K106 and Certain D009 wastes. In: Arsenic and Mercury – Removal, Recovery, Treatment, and Disposal. U.S. EPA. Noyes Data Corporation, Park Ridge, New Jersey, U.S.A, pp. 100–102.
Foord, E.E., Berendsen, P., Storey, L.O., 1974. Corderoite, first natural occurrence of $Hg_3S_2Cl_2$ from the Gordero mercury deposit, Humboldt County, Nevada. Am. Mineral. 59, 652–655.
Frueh, A.J., Grey, N., 1968. Confirmation and refinement of the structure of $Hg_3S_2Cl_2$. Acta Crystallogr. B24, 156–157.
Hagemoen, S.W., Condemine, A., Rockandel, M.A., 1994. The "REMERC" Process for Threatment of K106 Mercury Mud. Annual Meeting, Washington, DC (March 21–24, 1994), P35-. Chlorine Institute Inc, 9403, pp. 1–5.
Hammersley, A., 2004. Fit2D Version 12.034 (ESRF). Available at. www.esrf.fr/computing/scientific/FIT2D/index.html Last accessed 11 2009.
Kim, C.S., Brown Jr., G.E., Rytuba, J.J., 2000. Characterization and speciation of mercury-bearing mine wastes using X-ray absorption spectroscopy. Sci. Total Environ. 261, 157–168.
Kim, C.S., Bloom, N.S., Rytuba, J.J., Brown Jr., G.E., 2003. Mercury speciation by X-ray absorption fine structure spectroscopy and sequential chemical extractions: a comparison of speciation methods. Environ. Sci. Technol. 37, 5102–5108.
Kirpichtchikova, T.A., Manceau, A., Spadini, L., Panfili, F., Marcus, M.A., Jacquet, T., 2006. Speciation and solubility of heavy metals in contaminated soil using X-ray microfluorescence, EXAFS spectroscopy, chemical extraction, and thermodynamic modelling. Geochim. Cosmochim. Acta 70, 2163–2190.
Lodenius, M., Tulisalo, E., 1984. Environmental mercury contamination around a Finnish chlor-alkali plant. Bull. Environ. Contam. Toxicol. 32, 439–444.
Lowry, G.V., Shaw, S., Kim, C.S., Rytuba, J.J., Brown Jr., G.E., 2004. Macroscopic and microscopic observations of particle-facilitated mercury transport from New Idria and Sulphur Bank mercury mine tailings. Environ. Sci. Technol. 38, 5101–5111.
Malinowski, E.R., 1978. Theory of error for target factor analysis with applications to mas spectrometry and nuclear magnetic resonance spectrometry. Anal. Chim. Acta 103, 339–354.
Maserti, B.E., Ferrara, R., 1991. Mercury in plants, soil and atmosphere near a chlor-alkali complex. Water Air Soil Pollut. 56 (1), 15–20.
McCormack, J.K., 2000. The darkening of cinnabar in sunlight. Miner. Deposita 35, 796–798.
Mikac, N., Foucher, D., Niessen, S., Fischer, J.-C., 2002. Extractability of HgS (cinnabar and metacinnabar) by hydrochloric acid. Anal. Bioanal. Chem. 374, 1028–1033.
Neculita, C.M., Zagury, G.J., Deschênes, L., 2005. Mercury speciation in highly contaminated soils from chlor-alkali plants using chemical extractions. J. Environ. Qual. 34, 255–262.
Oram, L.L., Strawn, D.G., Marcus, M.A., Fakra, S.C., Möller, G., 2008. Macro- and microscale investigation of selenium speciation in Blackfoot River, Idaho sediments. Environ. Sci. Technol. 42 (18), 6830–6836.
Paquette, K., Helz, G., 1995. Solubility of cinnabar (red HgS) and implications for mercury speciation in sulfidic waters. Water, Air Soil Poll. 80, 1053–1056.
Quejido, A.J., Cozar, J.S., Pérez del Villar, L., Galan, M.P., Crespo, M., Fernandez-Diaz, M., Sanchez, M., 2002. Sequential leaching methods: review, previous experiences and proposed method for Fe(III)-U(VI)-rich fracture filling materials. Trends Geochem. 2, 19–42.
Ravel, B., Newville, M., 2005. ATHENA, ARTEMIS, HEPHAESTUS: data analysis for X-ray absorption spectroscopy using IFEFFIT. J. Synchrotron Rad. 12, 537–541.
Ravel, B., 2007. Artemis Manual Available at. http://cars9.uchicago.edu/~ravel/software/doc/Artemis/artemis.pdf Available atLast accessed 11 2009.
Ressler, T., Wong, J., Roos, J., Smith, I.L., 2000. Speciation of manganese particles in exhausted fumes of cars utilizing MMT. Environ. Sci. Technol. 34, 950–958.
Ressler, T., 1998. WinXAS: a XAS data analysis program under MS Windows. J. Synch. Rad. 5, 118–122.
Revis, N.W., Osborne, T.R., Holdsworth, G., Hadden, C., 1989. Distribution of mercury species from a mercury-contaminated site. Water Air Soil Pollut. 45, 105–113.
Sánchez, D.M., Quejido, A.J., Fernández, M., Hernández, C., Schmid, T., Millán, R., González, M., Aldea, M., Martín, R., Morante, R., 2005. Mercury and trace element fractionation in Almaden soils by application of different sequential extraction procedures. Anal. Bioanal. Chem. 381, 1507–1513.
Santoro, A., Terzano, R., Spagnuolo, M., Fiore, S., Morgana, M., Ruggiero, P., 2010. Mercury distribution in soils and plants surrounding an industrial area in the South of Italy. Int. J. Environ. Waste Manage. 5, 79–92.
Sass, B.M., Salem, M.A., Smith, L.A., 1994. Mercury Usage and Alternatives in the Electrical and Electronics Industries. Final Report. EPA/600/R-94/047. U.S. Environmental Protection Agency, Cincinnati, Ohio.
Scheinost, A.C., Kretzschmar, R., Pfister, S., 2002. Combining selective sequential extractions, X-ray absorption spectroscopy, and principal component analysis for quantitative zinc speciation in soil. Environ. Sci. Technol. 36, 5021–5028.
Senesi, N., D'Orazio, V., Ricca, G., 2003. Humic acids in the first generation of EUROSOILS. Geoderma 16, 325–334.
Singer, D.M., Zachara, J.M., Brown Jr., G.E., 2009. Uranium speciation as a function of depth in contaminated Hanford sediments – A micro-XRF, micro-XRD, and micro- and bulk-XAFS study. Environ. Sci. Technol. 43 (3), 630–636.
Slowey, A.J., Rytuba, J.J., Brown Jr., G.E., 2005. Speciation of mercury and mode of transport from Placer gold mine tailings. Environ. Sci. Technol. 39, 1547–1554.
Solé, V.A., Papillon, E., Cotte, M., Walter, P.H., Susini, J., 2007. A multiplatform code for the analysis of energy-dispersive X-ray fluorescence spectra. Spectrochim. Acta Part B 62, 63–68.
Spring, M., Grout, R., 2002. The blackening of vermilion: an analytical study of the process in paintings. Natl. Gallery Tech. Bull. 23 (1), 50–61.
Terzano, R., Spagnuolo, M., Vekemans, B., De Nolf, W., Janssens, K., Falkenberg, G., Fiore, S., Ruggiero, P., 2007. Assessing the origin and fate of Cr, Ni, Cu, Zn, Pb, and V in industrial polluted soil by combined microspectroscopic techniques and bulk extraction methods. Environ. Sci. Technol. 41 (19), 6762–6769.
Toby, B.H., 2001. EXPGUI, a graphical user interface for GSAS. J. Appl. Crystallogr. 34, 210–213.
Twidwell, L.G., Thompson, R.J., 2001. Recovering and recycling Hg from chlor-alkali plant wastewater sludge. JOM – J. Minerals, Metals Mater. Soc. 53 (1), 15–17.
Ullrich, S.M., Ilyushchenko, M.A., Kamberov, I.M., Tanton, T.W., 2007. Mercury contamination in the vicinity of a derelict chlor-alkali plant. Part I: sediment and water contamination of Lake Balkyldak and the River Irtysh. Sci. Total Environ. 381, 1–16.
USEPA, 1997. Mercury Study Report to Congress. In: Vol. III: Fate and Transport of Mercury into the Environment Available at. http://www.epa.gov/ttn/oarpg/t3/reports/volume3.pdf Last accessed 11 2009.
USEPA, 2007. Treatment Technologies for Mercury in Soil, Waste, and Water. U.S. Environmental Protection Agency Office of Superfund Remediation and Technology Innovation, Washington, DC. Available at. http://clu-in.org/download/misc/542r07003.pdf Last accessed 11 2009.
Vekemans, B., Janssens, K., Vincze, L., Adams, F., Van Espen, P., 1994. Analysis of X-ray spectra by iterative least squares (AXIL) – New developments. X-Ray Spectrom. 23, 278–285.
Webb, S.M., 2005. SIXPack: a graphical user interface for XAS analysis using IFEFFIT. Phys. Scr. vol. T115, 1011–1014.
Wyckoff, R.W.G., 1963. Crystal Structure 1, second ed. Interscience Publishers, New York, pp. 85–237.
Xia, K., Skyllberg, U.L., Bleam, W.F., Bloom, P.R., Nater, E.A., Helmke, P.A., 1999. X-ray absorption spectroscopic evidence for the complexation of Hg(II) by reduced sulfur in soil humic substances. Environ. Sci. Technol. 33, 257–261.
Yue, G.F., Wu, H.T., Jiang, X., He, W.X., Qing, C.L., 2006. Relationships between humic substance-bound mercury contents and soil properties in subtropical zone. J. Environ. Sci. 18 (5), 951–957.
Zagury, G.J., Neculita, C.M., Bastien, C., Deschenes, L., 2006. Mercury fractionation, bioavailability, and ecotoxicity in highly contaminated soils from chlor-alkali plants. Environ. Toxicol. Chem. 25, 1138–1147.